Visible-Light-Initiated Free-Radical Polymerization by Homomolecular Triplet-Triplet Annihilation

Nancy Awwad, Anh Thy Bui, Evgeny O. Danilov, Felix N. Castellano

Visible-Light Initiated Free Radical Polymerization by Homomolecular Triplet-Triplet Annihilation

Nancy Awwad, Anh-Thy Bui,[‡] Evgeny O. Danilov, and Felix N. Castellano*

Department of Chemistry, North Carolina State University, Raleigh, NC 27695-8204, USA.

[‡]Current Address: Univ Rennes, Ecole Nationale Supérieure de Chimie de Rennes, CNRS, ISCR – UMR6226, F-35000 Rennes, France.

Lead Contact: fncastel@ncsu.edu
Co-authors: nawwad@ncsu.edu, athy.bui@gmail.com , danilov@ncsu.edu

Summary

Polymerization reactions initiated by ultraviolet light are ubiquitous in scores of industrial applications but would markedly benefit from visible light activation to overcome stability, energy consumption, light penetration, and sample geometry limitations. The current work leverages visible-light driven homomolecular triplet-triplet annihilation (TTA) in zinc(II) meso-tetraphenylporphyrin (ZnTPP) to initiate facile free-radical polymerization in trimethylolpropane triacrylate (TMPTA) monomers through ultrafast electron transfer quenching. Selective Q-band (S_1) excitation of ZnTPP in the green or yellow (λ_{ex} = 514.5 or 552 nm) sensitizes TTA occurring between two ^{3}ZnTPP* energized chromophores, ultimately generating the highly reducing S_2 excited state on one ZnTPP molecule (E_{red} = -2.13 V *vs* SCE). Subsequently, this S_2 state engages in electron transfer with TMPTA or methyl acrylate (MA), thereby initiating the radical polymerization process. Estimation of the free energy of the reaction combined with electrochemistry strongly suggest that electron transfer is only plausible from the S_2 excited state of ZnTPP. Consistent with this hypothesis, the S_1 and T_1 excited states of ZnTPP showed no evidence of static or dynamic quenching by TMPTA. The bimolecular electron transfer was then verified by concentration-dependent dynamic fluorescence quenching of the ZnTPP S_2 excited state using optically gated fluorescence upconversion measurements. In acetonitrile, this electron transfer was concentration-dependent, with time constants ranging between 2.57 ps to 1.04 ps, with TMPTA concentrations from 0 to 3.47 M, respectively. The dynamic bimolecular quenching rate constant (9.5×10^{11} $M^{-1}s^{-1}$, in toluene) was in the same order of magnitude with that obtained from static fluorescence measurements (3.2×10^{11} $M^{-1}s^{-1}$, in toluene). FT-IR spectroscopy confirmed visible light-initiated polymerization through

monitoring consumption of the olefins in TMPTA as a function of photolysis time. EPR experiments, in conjunction with trapping radical species with 2-methyl-2-nitrosopropane (*t*-BuNO), identified that acrylate radicals were indeed formed through green light activation. Furthermore, we demonstrate that acrylate polymers of various macroscopic shapes as well as micron-scale objects can be produced using numerous low power visible light sources in the presence of only ZnTPP and TMPTA. These well-defined images represent the general applicability of homomolecular TTA mediated photoinitiated polymerization in both micro- and macro-fabrication applications.

1. Introduction

Photoinduced free radical polymerization represents a rapidly expanding "green" technology due to its solvent-free formulations, energy efficiencies, and modest reaction temperatures.[1-3] Radical polymerization often involves a photoinitiator to produce reactive species capable of converting a variety of monomers into a growing macromolecule in order to generate high-molecular-weight polymeric solids.[4] Trimethylolpropane triacrylate (TMPTA), a trifunctional acrylate monomer which produces highly crosslinked polymers with low toxicity, is excellent for many industrial applications.[5] When subjected to ultraviolet (UV) light (< 350 nm) or an electron beam, TMPTA used in conjunction with a photoinitiator rapidly polymerizes double bonds contained in nearby molecules.[5] However, exposure to highly energetic UV light is not ideal for biomedical applications,[6, 7] as it leads to degradation of the initiators, end-groups of the reversible addition-fragmentation chain transfer (RAFT) agents and/or can trigger monomer self-initiation processes.[8] Consequently, visible light mediated TMPTA-polymerization is necessary in

order to circumvent the obstacles associated with conventional UV-light initiated polymerization.[9] In fact, photoinitiators operating through visible light activation[10-12] are crucial for many industrial applications including dental restorative materials,[13, 14] photoresists,[15] laser-induced 3D curing,[16] integrated circuits,[10] printing plates,[17] and nanoscale micromechanics.[9] Yet, the design and usage of suitable photoinitiators that exploit visible light (λ > 380 nm) remain underexplored.[10-12, 18]

In recent years, porphyrins and metalloporphyrins derivatives have been investigated as visible light absorbing photoinitiators for free radical polymerization processes. It has been demonstrated that porphyrin derivatives can successfully promote excited state electron transfer chemistry,[19, 20] conduct cationic[21] or living anionic[22] polymerization, and activate living radical polymerization in the presence of RAFT agents.[19, 23-27] Previously, the S_1 and T_1 excited states of the zinc(II) meso-tetraphenylporphyrin (ZnTPP) have been leveraged to promote free radical polymerization. Al Mousawi *et. al.* proposed triplet and singlet excited state pathways for the electron transfer reaction occurring between ZnTPP and an iodonium salt for the polymerization of epoxides.[21] Likewise, Shanmugam *et. al.* suggested that the photoinduced electron transfer can take place from the triplet excited state of the ZnTPP to RAFT agents, resulting in the production of radicals to initiate polymerization.[23]

While porphyrin-based photoinitiators have been exploited in this regard, current formulations often require the presence of numerous additives to function.[28] To the best of our knowledge, the use of ZnTPP as a photoredox catalyst in free radical polymerization in the absence of any co-initiators, additives, or RAFT agents has never been reported. The proposed approach based on photochemical upconversion offers a

simple and cost-effective strategy, while limiting the number of components to two. However, activation of photoinduced polymerization that utilizes either heteromolecular or homomolecular triplet fusion has not been considered and mechanistically studied. In particular, exploiting homomolecular TTA can limit the photoinitiating system to a single component suitable for generating the free radicals necessary for subsequent polymerization and can potentially lead to a slower and controlled growth process which would change the very nature of the resultant soft materials. Homomolecular TTA from numerous metalated porphyrins is already well established,[29, 30] even in ZnTPP,[29, 31, 32] wherein two excited porphyrin triplets, ^{3}ZnTPP*, engage in bimolecular triplet-triplet energy transfer, ultimately generating the S_2 excited porphyrin.[31] This process is simply the homomolecular analog of photochemical upconversion based on sensitized TTA where the sensitizer and acceptor molecules are different.[33, 34] Although polymerization of methyl methacrylate (MMA) facilitated by the heteromolecular photochemical upconversion containing numerous additives has been recently demonstrated, no mechanistic details were provided.[35] Generally speaking, the potential scope of photoactivating free radical polymerization using TTA mechanisms in conjunction with visible light input is extraordinary as the excited state reducing power that can be achieved is truly impressive and a number of representative super-reductant TTA compositions have been recently reviewed.[36]

In this report, homomolecular triplet-triplet annihilation (TTA) using ZnTPP is explored as a new photo-initiating mechanism for the free radical polymerization of triacrylates and methyl acrylate using long wavelength visible light. We provide substantial mechanistically relevant details related to the polymerization of TMPTA

following selective monochromatic Q-band (S_1) excitation of ZnTPP in the green using only these two components. Through an array of spectroscopic techniques, we provide compelling evidence that the S_2 excited state of ZnTPP engages in dynamic electron transfer with TMPTA and methyl acrylate (MA). We demonstrate that the S_2 state of ZnTPP, rather than S_1 or T_1, is exclusively responsible for promoting free radical polymerization. Furthermore, EPR and FT-IR spectroscopy provided experimental confirmation of both radical formation and olefin consumption in TMPTA resulting from utilizing visible light excitation. Numerous plastic objects of varying dimensions were readily produced from green and yellow light activation (500 - 600 nm) in both macroscopic and microscopic size regimes.

2. Results and Discussion

2.1. Static Spectroscopic Properties of ZnTPP and TMPTA

The chemical structures of the ZnTPP and TMPTA are provided in **Figure 1A**. Prior to investigating the TTA mechanism of the photoinduced polymerization, steady-state absorption and fluorescence emission characteristics of the ZnTPP and TMPTA were examined individually. The normalized UV-Vis absorption and fluorescence spectra of ZnTPP in toluene is presented in **Figure 1B**. As illustrated in **Figure 1B**, the absorption spectrum of ZnTPP exhibits two characteristic electronic transitions centered near 425 and 550 nm. In accordance with previous reports,[29, 37, 38] these transitions have been assigned to Soret- ($S_0 \rightarrow S_2$) and Q- ($S_0 \rightarrow S_1$) bands, respectively. It is noteworthy that a monochromatic excitation at 514.5 nm using an Ar^+ laser resulted in two distinct fluorescence transitions attributed to $S_1 \rightarrow S_0$ and $S_2 \rightarrow S_0$, the latter being anti-Stokes in

nature. These fluorescence bands are mirror images of the Q- and Soret- bands of the ZnTPP absorption spectrum, respectively.[29, 38] Fluorescence emanating from an upper excited state is a unique attribute of the ZnTPP, and is one of the few exceptions that violates Kasha's rule.[39] Considering that the Soret-band of ZnTPP cannot be excited directly using a 514.5 nm excitation source, the S_2 state was formed solely as a result of bimolecular TTA, $2T_1 \rightarrow S_2 + S_0$.[29, 32, 40] While ZnTPP displays various absorption and emission features across the entire visible range, TMPTA exhibits only one high energy absorption band centered at ~275 nm , **Figure 1C**. Moreover, the addition of TMPTA to the solution of ZnTPP does not significantly modify the profile of the ZnTPP absorption spectrum. The lack of change to this absorption envelope indicates the absence of any ground state complexation between ZnTPP and TMPTA.

As proof-of-concept, the Q band of ZnTPP was excited using bandpass filtered 514.5 nm output from an Ar^+ laser and 532 nm output from a laser pointer respectively, in a solution of 5×10^{-5} M ZnTPP and 2.47 M TMPTA in degassed media and clearly resulted in polymerization (see **Video S1** which illustrates the latter). Also, given the quadratic excitation power dependence of the homomolecular TTA process in the weak annihilation limit, polymerization was further verified at low light fluxes using both coherent and non-coherent light sources in order to invoke the TTA mechanism as being operative for promoting free radical polymerization (**Figures S1 and S2**).

2.2. Feasibility of Excited State Electron Transfer

Electron transfer from the photoinitiator to the monomer is of fundamental importance in radical generation for photoinitiated polymerization. Furthermore, the aforementioned radical generation following TTA relies on the electron donating ability of

the S_2 excited state of ZnTPP. Hence, it is critical to assess the feasibility of electron transfer utilizing this state. The driving force (ΔG_{et}) and redox potentials for the various electron transfers involving distinct excited states (S_1, T_1, and S_2) of ZnTPP were estimated using the redox potentials of the porphyrins and acrylate quenchers. For the latter, we used the established reduction potential of MA as a surrogate for TMPTA which could not be accurately measured due to its propensity for rapid polymerization upon reduction. Therefore, the ΔG_{et} values for all possible reactions between ZnTPP and TMPTA were estimated using the Rehm-Weller expression,[41] ignoring the work terms since polar solvents were used[42] (**Equation 1)**.

$$\Delta G_{et} = E_{ox}(D) - E_{red}(A) - E^* \qquad \textbf{(1)}$$

$E_{ox}(D)$ and $E_{red}(A)$ are the oxidation and reduction potentials of the ZnTPP donor and the MA acceptor in CH_3CN. E^* represents the energy of each relevant excited state in ZnTPP. The energies of the S_1 and S_2 states were approximated from the fluorescence spectra presented in **Figure 1B**, consistent with literature values,[43] and the T_1 energy was previously reported by Harriman and coworkers.[44] The relevant redox potentials of ZnTPP and MA as well as estimates of the ΔG_{et} values are summarized in **Table 1**. The estimated ΔG_{et} values for S_1, T_1, and S_2 are 0.83 V, 1.31 V and -0.035 V, respectively. The excited state redox potentials, $E(M^+/M^*)$, of the S_1, T_1, and S_2 states of ZnTPP were calculated according to the modified Rehm-Weller equation for excited state redox potentials.[45] The potentials of the S_1, T_1 and S_2 states of ZnTPP were calculated as -1.67 V, -1.19 V and -2.53 V, respectively. Moreover, the reduction potential of the MA in CH_3CN was previously reported as $E_{red}(MA)$ = -2.1 V vs SCE.[46]

Taken together, assessments of ΔG_{et} values and the excited state oxidation potentials predict that the photoinduced electron transfer from ZnTPP to MA, and consequently TMPTA, is indeed feasible and favorable *only* from the S_2 excited state. Instances of the electron transfer involving upper excited states is rather under-documented due to the rapid internal conversion rate experienced in many molecular systems.[48] On the contrary, Zn(II) porphyrins have relatively slow and inefficient internal conversion[48-53] in addition to a large $S_0 \rightarrow S_2$ transition dipole moment.[54, 55] As a result, producing a high-energy S_2 state of ZnTPP through TTA that is capable of transferring an electron to a nearby acceptor has been the subject of several recent reports.[53, 56, 57]

2.3. Quenching of the Excited States in ZnTPP

Once the feasibility of electron transfer from the S_2 state of ZnTPP was verified, quenching of the ZnTPP excited states (S_1, T_1, and S_2) was investigated through a combination of fluorescence (S_1 and S_2) and transient absorption (T_1) studies in the presence of acrylates. First, fluorescence spectra of the ZnTPP were collected using various concentrations of TMPTA in aerated toluene upon direct excitation of the Soret-band at 400 nm; the aerated conditions were necessary to avoid initiating polymerization. The emission transitions with band maxima at 432 nm and 550 – 750 nm correspond to the S_2 and S_1 fluorescence, respectively, after subtraction of the Raman bands measured in pure toluene and TMPTA/toluene mixtures in the absence of ZnTPP. In the event of TTA mediated electron transfer, only the S_2 state serves as the electron donor in the ZnTPP-acrylate system. Consequently, this electron transfer is accompanied by a quenching of the S_2 fluorescence in ZnTPP, whereas the S_1 fluorescence remains

unperturbed.[57] This behavior is clearly illustrated in **Figure 3A**, where the S_2 fluorescence emission of ZnTPP exhibits significant quenching in the presence of TMPTA whereas the S_1 fluorescence does not, **Figure 3B**. Moreover, the degree of S_2 fluorescence quenching exhibited a clear correlation with the TMPTA concentration.

To evaluate the concentration dependence on fluorescence quenching, Stern-Volmer analyses were conducted on both the S_2 and S_1 emission bands of ZnTPP in the presence of TMPTA, ultimately yielding the fluorescence quenching rate constant of the S_2 excited state. Stern-Volmer plots of the S_2 and S_1 emission bands are displayed in **Figure 3C**. The S_2 data revealed a positive linear slope, featuring a large bimolecular quenching constant (k_q) of 3.2×10^{11} M^{-1} s^{-1}; k_q was calculated using the S_2 excited state lifetime of ZnTPP (1.51 ps). However, the Stern-Volmer plot of the S_1 state displayed negligible changes across all TMPTA concentrations measured, indicating no evidence of quenching.

In addition, following the analysis of Tipathy *et. al.* examining the effect of excited state polarizabilities in different solvents, the values of Lorenz-Lorentz polarizability functions calculated using the refractive indices n of toluene (f_1 = 0.296, n = 1.503) and TMPTA (f_1 = 0.281, n = 1.474) show a decrease as a function of the increasing S_2-S_1 energy gap, reflecting an opposite trend to the S_2 emission quenching observed in ZnTPP.[58] Thus, there is no evidence that metal polarizability has any significant effect on the S_2 population decay dynamics of ZnTPP and the S_2 emission quenching observed in TMPTA is exclusively due to excited state electron transfer.

Furthermore, the possibility of photoinduced electron transfer from the triplet excited state of ZnTPP (^{3}ZnTPP*) was also evaluated. Due to the non-emissive nature of ^{3}ZnTPP*, an analogous excited state quenching experiment employing transient absorption spectroscopy was necessary here. Transient absorption difference spectra in the visible region were recorded as presented in **Figure S3,** where the Q-band of ZnTPP was excited using 550 nm laser pulses in the presence of increasing concentrations of TMPTA in aerated toluene to prevent initiating polymerization.

Immediately following the laser pulse, the excited state absorption band ($T_1 \rightarrow T_n$)[59, 60] appeared at 465 nm, which is attributed to ^{3}ZnTPP*.[61-63] Interestingly, the magnitude of the prompt ^{3}ZnTPP* transient features experienced negligible changes as a function of TMPTA concentration. The decay curves of ^{3}ZnTPP* measured at 465 nm (**Figure S4A**) obeyed first-order kinetics and displayed an *increase* in the lifetime of ^{3}ZnTPP* as more TMPTA was added. This trend is reflected in the Stern-Volmer analysis shown in **Figure S4B**, where a negative K_{SV} value was obtained, indicative of an anti-quenching process. This result is partially due to oxygen solubility changing as a function of sample composition, which is reported to be [O_2] ~1 mmol/L in TMPTA[64] while it is [O_2] ~2 mmol/L in toluene.[65] Also, considering that oxygen is an effective scavenger for triplet excited states in aerated solutions, the oxygen quenching rate is closely related to the diffusion limit set by the viscosity of the solvent. With that in mind, this unexpected negative Stern-Volmer slope is attributed to a viscosity effect, as increasing TMPTA leads to marked increases in the viscosity of the solution. Higher viscosity reduces the effect of oxygen quenching, thereby leading to an apparent increase in the lifetime of ^{3}ZnTPP*. To validate this interpretation, the photoluminescence of the singlet oxygen ($^1O_2$) at 1270 nm[66]

sensitized by ^{3}ZnTPP* was measured. Upon 550 nm excitation, the $^{1}O_2$ emission intensity at 1270 nm decreased as a function of increasing TMPTA concentration, **Figure S5**. These results confirm that viscosity, and consequently, the extent of oxygen diffusion, was responsible for the TMPTA anti-quenching process observed from T_1. It is noteworthy that bimolecular processes have been demonstrated to benefit from the extended triplet lifetimes available in solvents of high viscosity.[67] It is conceivable that TTA-initialized polymerization may be improved owing to such viscosity effects. Overall, the combined quenching results support excited state electron transfer emanating from S_2 in ZnTPP.

2.4. Polymer Gel Formation and Radical Generation Through Electron Transfer

In degassed two-component mixtures of TMPTA (3.7 M) with ZnTPP (5×10^{-5} M), polymer gels were immediately produced when the S_2 state was directly excited at 427 nm (28 mW/cm^2). To circumvent the practical limitations of working with degassed media, 10^{-2} M dimethylfuran (DMF) was incorporated as an oxygen scavenger in the photoresist to simplify the experimental format.[66] Since a C=C bond is consumed during polymerization, the progress of gel formation was monitored (**Table S1**) using its characteristic vibration at 1635 cm^{-1} in the TMPTA IR spectrum.[68] With IR spectra normalized to the C=O band at 1725 cm^{-1},[69] the absorbance of the C=C bonds at 1635 cm^{-1} decreases with increasing 427 nm exposure time, indicating that the TMPTA monomer is being consumed as a result of S_2 photoactivation, **Figure 4**.

Moreover, the free radical generation necessary for polymerization was further examined using electron paramagnetic resonance (EPR) spectroscopy of degassed

ZnTPP-MA solutions (1.3 x 10^{-4} M ZnTPP in 1:1 MA/ toluene mixture) irradiated with green light. Once again, MA was used in place of TMPTA to prevent rapid polymerization of these mixtures in the EPR tube. The resulting EPR spectrum of ZnTPP-$MA^{\bullet -}$ generated using Q-band (S_1) excitation at 514.5 nm exhibits three well-resolved hyperfine lines, which was readily simulated using a slow-motion algorithm (a_H = 15.32 G), **Figure 5A**. Hence, the three-line hyperfine structure arises due to the interaction between the unpaired electron and the protons of methylene groups of the $MA^{\bullet -}$, and is consistent with that reported in the literature.[70, 71] In addition, the hyperfine structure corresponding to $MA^{\bullet -}$ appears only in the presence of the ZnTPP and light excitation. Neither ZnTPP nor the acrylate gives a measurable EPR spectrum when exposed to visible light.

Using 2-methyl-2-nitrosopropane (*t*-BuNO), the free radicals in the propagating MA chain can be captured. The transient MA radicals react with *t*-BuNO and produce stable nitroxide radicals which exhibit a primary triplet hyperfine coupling (intensity, 1:1:1) from the ^{14}N (I = 1) of the nitroxide group. Previously, EPR spectra from the trapping of methacrylate radicals, such as MA and methyl methacrylate (MMA) (**Figure S6)**, using *t*-BuNO have been reported by Kunitaki and Murakami with azobisisobutyronitrile (AIBN) as an initiator.[72] By comparing the hyperfine splitting EPR signatures of the stable nitroxide radicals formed with AIBN using UV excitation to those generated using ZnTPP with visible light, the structures of the trapped radicals can be readily identified. As anticipated, the EPR spectrum produced in the AIBN—MA—*t*-BuNO system (**Figure 5B**) displays quantitative resemblance to the three-line spectrum of the trapped species formed in the ZnTPP—MA—*t*-BuNO system. These observations illustrate that the

acquired EPR spectrum stems from radicals in the propagating MA polymeric chains that were originally formed as a result of *electron transfer* from the S_2 excited state of ZnTPP.

2.5. Dynamics of the S_2 Intermediate

The S_2 excited state of ZnTPP has been shown as the key intermediate bridging TTA and electron transfer, where its population decay directly informs on the reactive radical generation that initiates the polymerization process. Hence, real-time dynamics of Soret-excited ZnTPP were recorded with using an optically gated fluorescence upconversion apparatus in the presence of acrylate quenchers to glean further insight into the dynamics of this quenching. In order to stabilize the radical-ion pair formed from the electron transfer,[73] acetonitrile (CH_3CN) was selected. Additionally, using CH_3CN extends the lifetime of the S_2 excited state with respect to toluene, enabling more efficient electron transfer.[73] However, the results acquired in toluene (**Figures S7 and S8**) were qualitatively similar to those obtained in CH_3CN.

Figure 6A presents the S_2 fluorescence transients of ZnTPP monitored at 435 nm (λ_{ex} = 400 nm), measured as a function of TMPTA concentration (0 to 3.47 M). It is apparent that the S_2 decay accelerates with increasing quencher concentration, consistent with dynamic quenching. In the absence of the TMPTA, the S_2 dynamics are best described as a single-exponential decay with a lifetime of 2.57 $\pm$ 0.03 ps, which is in close agreement with previous studies.[57, 74] On the contrary, when the TMPTA was added, a sum of two exponential functions that incorporate two time-components (τ_D^F and τ_D^S) was necessary to adequately model the resultant intensity decay dynamics. The τ_D^S corresponds to the lifetime of the S_2 state of ZnTPP in pure CH_3CN (2.57 ps) which was

fixed in this analysis. This procedure enabled a single time constant to be determined across the entire series of quencher concentrations. Additionally, the amplitudes of each time component, A_D^F and A_D^S, represent the relative contributions of τ_D^F and τ_D^S to the overall decay, respectively. For example, when [TMPTA] = 3.47 M, a lifetime (τ_D^F) of 1.04 ps was determined, which accounted for 81% of the total intensity decay amplitude. This fitting procedure echoes previous work where time constants were measured for excited state electron transfer from the S_2 excited state of ZnTPP in CH_3CN.[57] The time constant components, τ_D^F and τ_D^S, obtained from the complete analysis in CH_3CN are collected in **Table S2,** as well as in toluene, **Table S3**.

The dynamic Stern−Volmer plot (**Figure 6A, inset**) was generated from the measured values of τ_D^F listed in **Table S2.** This ultrafast quenching process obeys the Stern–Volmer relation as indicated by the linearity witnessed across the entire range of quencher concentrations. This analysis revealed a Stern−Volmer constant ($K_{SV} = k_q \tau_D^F{}_0$) of 0.423 M^{-1} which corresponded to a bimolecular quenching rate constant (k_q) of 1.6×10^{11} M^{-1} s^{-1}. The obtained k_q value is of the same magnitude with that obtained from static fluorescence measurements. The dynamic quenching process is consistent with exothermic excited state electron transfer from the S_2 excited state of ZnTPP to TMPTA forming $TMPTA^{\bullet-}$.

Although electron transfer from the S_2 state of ZnTPP has now been corroborated, this particular experiment directly pumped S_2 using blue light. To illustrate that an electron can be transferred following homomolecular TTA, the static upconverted S_2 emission spectra were recorded through selective excitation of the Q-band excitation using degassed solutions of the acrylate quencher in toluene. Since these TTA experiments

needed to be performed in the absence of oxygen, and rapid polymerization of TMPTA occurs under these conditions, MA was once again used as a surrogate quencher. The upconverted S_2 fluorescence of ZnTPP was efficiently quenched by MA and exhibited a subtle blue shift (ca. 2 nm) which was directly correlated with the proportion of MA in the mixture, **Figure 6B**. This blue-shifted S_2 fluorescence in ZnTPP resulted from the increased polarity of the solution upon addition of the liquid MA quencher, as recognized in solvent polarity studies.[29-32] Analogous to the behavior witnessed from direct Soret-band excitation, the Stern-Volmer plot of the upconverted S_2 fluorescence revealed quenching by MA with a K_{sv} = 1.19 M^{-1} (**Figure 6B, inset**). This K_{sv} translates to a quenching rate constant of 7.9×10^{11} M^{-1} s^{-1}, given that lifetime of the ZnTPP S_2 state measured in toluene is 1.51 ps. It is noteworthy that although the S_2 fluorescence is quenched by MA following visible light activation, the S_1 fluorescence was completely invariant to the MA concentration (**Figure S9**). These results further endorse the proposed mechanism of homomolecular TTA induced free radical polymerization following selective visible excitation into the ZnTPP Q-band.

2.6. Microfabrication

Once the mechanisms involving TTA activated photoinduced polymerization were elucidated, the applicability and the broad utility of this method were given consideration. Using a confocal laser scanning microscope equipped with various low-energy light sources, we patterned a variety of micron-sized objects. To prevent triplet quenching when working with degassed media, dimethylfuran (DMF) was incorporated as an oxygen scavenger.[66] As proof-of-concept, a mixture of ZnTPP (5×10^{-5} M) in TMPTA (3.7 M) and

DMF (10^{-2} M) was illuminated through a photomask (a TEM grid) for 1-minute of exposure, using a short wavelength-filtered halogen lamp (λ_{ex} > 455 nm, ~1 W/cm^2) in order to selectively excite the Q-band of ZnTPP. The *in-situ* bright-field image (**Figure 7A**) generated with a 458 nm Ar^+ laser line to avoid exciting the initiator features well-defined two-dimensional grid patterns obtained after 2-minute exposure. Furthermore, as presented in **Figures 7 B, C, D**, numerous representative objects were microfabricated using another available low energy photon light source (561 nm diode pumped solid state laser, ~10^5 W/cm^2, laser scan speed 21 mm/s) within this microscope.

Due to the growing interest towards downscaling and miniaturizing macroscopic products in many industries, there are an increasing number of attempts to develop micro- and nanoscale fabrication processes.[75] These microscopic products are desired for various applications in the fields of medical, optics, automotive, electronics, and biotechnology. In recent years, there have been rapid improvements in microfabrication technologies which led to the development of highly functional applications such as biochips, micro/nano-fluidic devices, photonic crystals, and nano/micro-electromechanical systems (N/MEMS).[75, 76]

As outlined earlier, the majority of approaches to creating microscopic products via photoinduced polymerization rely on high energy laser sources. The microfabrication in this work illustrates that even low energy photon excitation sources may be used to induce polymerization, avoiding the detrimental effects often caused by high energy sources. The development of well-defined two-dimensional features, as in the images shown in **Figure 7,** constitutes a first step toward 3D microfabrication. However, fabrication of 3D microscopic structures remains challenging to accomplish, due to difficulties in controlling

polymerization in the z-direction through TTA-initiated polymerization. Moving forward, further examination of the spatial extent of polymerization will be necessary to explore the full potential of this exciting methodology.

Conclusion

To summarize, the mechanism of photoinduced polymerization of TMPTA units through long-wavelength visible-light activation based on homomolecular TTA using a ZnTPP photoinitiator was investigated. In this example, ZnTPP acts as both the sensitizer and upconverting emitter, where TTA results in the formation of the S_2 excited state of the porphyrin. Upon addition of an acrylate monomer, trimethylolpropane triacrylate (TMPTA), an electron is transferred from the S_2 excited state of ZnTPP to induce the polymerization, as supported by the associated thermodynamics. Moreover, a combination of concentration dependent fluorescence and transient absorption studies revealed that only the S_2 excited state was quenched by the acrylates investigated. Polymer gels generated from TMPTA were produced through either direct excitation of the Soret band (S_2 pumping) or Q-band stimulation (S_1), the latter leading to sensitized formation of the S_2 excited state. The identities of the radicals generated during the photoinitiated gel formation were examined using EPR measurements and they were found to be identical to those generated using UV light activation with AIBN. Fluorescence upconversion measurements were performed to monitor the dynamics of the S_2 excited state decay as a function of acrylate quencher concentration. The dynamics of the S_2 fluorescence accelerated with increasing acrylate quencher concentration, where this ultrafast quenching process obeyed the Stern–Volmer relation with a bimolecular quenching rate constant of $1.6 \times 10^{11}\ M^{-1}\ s^{-1}$, in good agreement with that obtained from

static fluorescence measurements. Furthermore, homomolecular TTA was used to sensitize the S_2 excited state resulting from Q-band excitation and the quenching of this upconverted emission echoed that resulting from Soret band excitation. These combined results leave little doubt that acrylate polymerization proceeds exclusively from the ZnTPP S_2 excited state, regardless if it is directly formed or sensitized through homomolecular TTA. Using this TTA-based photochemistry, precise microscopic structures were drawn using low power visible excitation sources. This could be particularly beneficial for applications requiring slow polymerization rates such as restorative dentistry and designer macromolecules with targeted mechanical properties. Homomolecular triplet fusion also promotes deep light penetration depth into the monomer solution enabling newly conceived applications in 3D printing using visible light. Hence, homomolecular TTA presents itself as an exciting new avenue for both major macroscopic plastic products (engineered polymers and coatings) as well as value added manufacturing of microscopic specialty plastics (microfluidics, needles, optics, etc.) thereby encompassing a comprehensive range of markets, and this contribution merely represents an introduction to this powerful photoactivation mechanism.

Experimental Procedures

Resource Availability

Lead Contact

Further information and requests for reagents should be directed to and will be fulfilled by the Lead Contact, (fncastel@ncsu.edu).

Materials Availability

Full experimental and spectroscopy measurements details can be found in the Supplemental Information.

Data and Code Availability

All data supporting this study are available in the manuscript and Supplemental Information.

SUPPLEMENTAL INFORMATION

Supplemental Information includes Supplemental Experimental Procedures, 9 figures, 3 tables, and 1 video and can be found with this article online at ...

Acknowledgement

We acknowledge support for this contribution from BioLEC, an Energy Frontier Research Center funded by the U.S. Department of Energy, Office of Science, Office of Basic Energy Sciences under Award No. DE-SC0019370. A.T.B. was supported by the U.S. Department of Energy, Office of Science, Office of Basic Energy Sciences, under Award Number DE-SC0011979. We thank Prof. Seth R. Marder at the Georgia Institute of Technology for suggesting TTA photochemistry in polymerization reactions.

AUTHOR CONTRIBUTIONS

Conceptualization, Experiments, Data Analysis and Writing, N.A.; Manuscript input and Laser Microfabrication Experiments, AT.B.; Assistance with Ultrafast Measurements, E.D.

DECLARATION OF INTERESTS

The authors declare no competing interests.

Legends

Table 1. Free Energies for Excited State Electron Transfer from ZnTPP*(S_1), ZnTPP*(T_1) and ZnTPP* (S_2) to MA.[a]

Solvent	E^*_{S1} (eV)	$\Delta G_{et}(S_1)$ (V)	E^*_{T1} (eV)	$\Delta G_{et}(T_1)$ (V)	E^*_{S2} (eV)	$\Delta G_{et}(S_2)$ (V)
CH_3CN	2.07[b]	+0.83[d]	1.59[c]	+1.31[d]	2.935[b]	-0.035[d]

[a] The ground state oxidation potential of 0.8 V vs SCE[47] for ZnTPP and reduction potential of −2.1 V vs. SCE[46] for MA were used to estimate the driving forces for the various electron transfer reactions with TMPTA. [b]From ref [43]. [c]From ref [44]. [d]Calculated from ***Eq. 1.***

Video S1. Output from a 532 nm green laser pointer (~100 mW) inducing polymerization in a mixture of 1.8 × 10^{-5} M ZnTPP with 2.47 M TMPTA in the presence of DMF and degassed toluene respectively.

Figure 1. Chemical structures of (A) zinc(II) *meso*-tetraphenylporphyrin (ZnTPP) and trimethylolpropane triacrylate (TMPTA). (B) Normalized absorption and fluorescence spectra of ZnTPP in degassed toluene. (C) Absorption spectra of a mixture of 3.3 × 10^{-6} M ZnTPP with 0.616 M TMPTA in degassed toluene. *Inset*: relative absorption intensities of ZnTPP vs. the ZnTPP/TMPTA mixture.

Figure 2. Representation of the excited state redox potentials of ZnTPP and MA obtained from their electrochemical analysis vs. Fc^+/ Fc in CH_3CN. Based on the excited state redox potentials, electron transfer is plausible only from the S_2 state of ZnTPP. It is assumed that the redox potential of TMPTA is identical to that of MA.

Figure 3. Static fluorescence quenching of (A) Soret-band and (B) Q-band emission of the ZnTPP with various amounts of TMPTA in toluene. (C) Stern-Volmer plot of the Soret-band (in blue) and Q-band (in red) emission. Soret-band experience emission quenching in the presence of TMPTA, whereas the Q-band does not.

Figure 4. The absorbance variance of C=C bonds in TMPTA gels at 1635 cm^{-1} with respect of normalized C=O absorbance upon increasing exposure time of visible

light (427 nm). Over time, absorbance of C=C decreases reflecting the progression of photoinduced polymerization. *Inset:* magnified C=C absorbance over exposure time.

Figure 5. (A) Experimental (red) and simulated (blue) EPR spectrum of MA radicals generated in the presence of ZnTPP upon irradiation. Simulated spectrum with a_H set to 15.32 G. (B) Comparison of *t*-BuNO trapped MA radicals with ZnTPP (red) and AIBN (blue) photoinitiators. These EPR spectra indicate the formation of $MA^{\bullet-}$.

Figure 6. (A) Normalized S_2 transient emission decay of the ZnTPP in CH_3CN monitored at 435 nm after Soret-band excitation with varying TMPTA concentration. *Inset*: Stern-Volmer plot generated from the S_2 excited-state lifetime quenching of the ZnTPP as a function of TMPTA concentration. (B) Quenching of the upconverted ZnTPP S_2 emission spectra in degassed toluene, after Q-band excitation as a function of increasing concentrations of MA. *Inset*: corresponding Stern-Volmer plot of the upconverted S_2 emission quenching by MA.

Figure 7. Optical images of objects polymerized using (A) a short-wavelength filtered halogen lamp with λ_{ex} > 455 nm (bright field, transmitted light: 458 nm) and (B), (C), (D) a 561 nm diode laser (DIC, transmitted light: 633 nm).

References

1. Davidson; Stephen, *Exploring the Science, Technology and Applications of UV and EB Curing*. SITA Technology LONDON, **1999**.
2. Allen, N., *Photochemistry and Photophysics of Polymer materials*. **2010**.
3. Fouassier, J.-P., *Photoinitiation, Photopolymerization, and Photocuring: Fundamentals and Applications*. Hanser: **1995**.
4. Rudin, A.; Choi, P., Chapter 8 - Free-Radical Polymerization. In *The Elements of Polymer Science & Engineering (Third Edition)*, Rudin, A.; Choi, P., Eds. Academic Press: Boston, **2013**; pp 341-389.
5. Kirkland, D.; Fowler, P., A review of the genotoxicity of trimethylolpropane triacrylate (TMPTA). *Mutation Research-Genetic Toxicology and Environmental Mutagenesis* **2018,** *828*, 36-45.
6. Liu, V. A.; Bhatia, S. N., Three-dimensional photopatterning of hydrogels containing living cells. *Biomedical Microdevices* **2002,** *4* (4), 257-266.
7. Burdick, J. A.; Padera, R. F.; Huang, J. V.; Anseth, K. S., An investigation of the cytotoxicity and histocompatibility of in situ forming lactic acid based orthopedic biomaterials. *Journal of Biomedical Materials Research* **2002,** *63* (5), 484-491.
8. Yeow, J.; Xu, J. T.; Boyer, C., Polymerization-Induced Self-Assembly Using Visible Light Mediated Photoinduced Electron Transfer-Reversible Addition-Fragmentation Chain Transfer Polymerization. *Acs Macro Letters* **2015,** *4* (9), 984-990.
9. Tehfe, M. A.; Louradour, F.; Lalevee, J.; Fouassier, J. P., Photopolymerization Reactions: On the Way to a Green and Sustainable Chemistry. *Applied Sciences-Basel* **2013,** *3* (2), 490-514.

10. Allen, N. S., Photoinitiators for UV and visible curing of coatings: Mechanisms and properties. *Journal of Photochemistry and Photobiology a-Chemistry* **1996,** *100* (1-3), 101-107.
11. Valdes-Aguilera, O.; Pathak, C. P.; Shi, J.; Watson, D.; Neckers, D. C., Photopolymerization studies using visible light photoinitiators. *Macromolecules* **1992,** *25* (2), 541-547.
12. Jakubiak, J.; Rabek, J. F., Photoinitiators for visible light polymerization. *Polimery* **1999,** *44*, 447-461.
13. Moszner, N.; Salz, U., New developments of polymeric dental composites. *Progress in Polymer Science* **2001,** *26* (4), 535-576.
14. Moszner, N.; Salz, U.; Zimmermann, J., Chemical aspects of self-etching enamel-dentin adhesives: A systematic review. *Dental Materials* **2005,** *21* (10), 895-910.
15. Moon, J. H.; Ford, J.; Yang, S., Fabricating three-dimensional polymeric photonic structures by multi-beam interference lithography. *Polymers for Advanced Technologies* **2006,** *17* (2), 83-93.
16. Fouassier, J. P.; MorletSavary, F., Photopolymers for laser imaging and holographic recording: Design and reactivity of photosensitizers. *Optical Engineering* **1996,** *35* (1), 304-312.
17. Hiller, J.; Mendelsohn, J. D.; Rubner, M. F., Reversibly erasable nanoporous anti-reflection coatings from polyelectrolyte multilayers. *Nature Materials* **2002,** *1* (1), 59-63.
18. Yagci, Y.; Jockusch, S.; Turro, N. J., Photoinitiated Polymerization: Advances, Challenges, and Opportunities. *Macromolecules* **2010,** *43* (15), 6245-6260.
19. Yeow, J.; Shanmugam, S.; Corrigan, N.; Kuchel, R. P.; Xu, J. T.; Boyer, C., A Polymerization-Induced Self-Assembly Approach to Nanoparticles Loaded with Singlet Oxygen Generators. *Macromolecules* **2016,** *49* (19), 7277-7285.
20. Kim, D. K.; Stansbury, J. W., A Photo-Oxidizable Kinetic Pathway of Three-Component Photoinitiator Systems Containing Porphrin Dye (Zn-tpp), an Electron Donor and Diphenyl Iodonium Salt. *Journal of Polymer Science Part a-Polymer Chemistry* **2009,** *47* (12), 3131-3141.
21. Al Mousawi, A.; Poriel, C.; Dumur, F.; Toufaily, J.; Hamieh, T.; Fouassier, J. P.; Lalevee, J., Zinc Tetraphenylporphyrin as High Performance Visible Light Photoinitiator of Cationic Photosensitive Resins for LED Projector 3D Printing Applications. *Macromolecules* **2017,** *50* (3), 746-753.
22. Sugimoto, H.; Kuroki, M.; Watanabe, T.; Kawamura, C.; Aida, T.; Inoue, S., High-Speed Living Anionic-Polymerization of Methacrylic Esters with Aluminium Porphyrin Initiators - Organoaluminium Compounds as Lewis-Acid Accelerators. *Macromolecules* **1993,** *26* (13), 3403-3410.
23. Shanmugam, S.; Xu, J. T.; Boyer, C., Exploiting Metalloporphyrins for Selective Living Radical Polymerization Tunable over Visible Wavelengths. *Journal of the American Chemical Society* **2015,** *137* (28), 9174-9185.
24. Dadashi-Silab, S.; Doran, S.; Yagci, Y., Photoinduced Electron Transfer Reactions for Macromolecular Syntheses. *Chemical Reviews* **2016,** *116* (17), 10212-10275.
25. Yeow, J.; Joshi, S.; Chapman, R.; Boyer, C., A Self-Reporting Photocatalyst for Online Fluorescence Monitoring of High Throughput RAFT Polymerization. *Angewandte Chemie-International Edition* **2018,** *57* (32), 10102-10106.

26. Reeves, J. A.; Watuthanthrige, N. D.; Boyer, C.; Konkolewicz, D., Intrinsic and Catalyzed Photochemistry of Phenylvinylketone for Wavelength-Sensitive Controlled Polymerization. *Chemphotochem* **2019,** *3* (11), 1171-1179.
27. Yeow, J.; Boyer, C., Photoinitiated Polymerization-Induced Self-Assembly (Photo-PISA): New Insights and Opportunities. *Advanced Science* **2017,** *4* (7).
28. Chen, M.; Zhong, M. J.; Johnson, J. A., Light-Controlled Radical Polymerization: Mechanisms, Methods, and Applications. *Chemical Reviews* **2016,** *116* (17), 10167-10211.
29. Stelmakh, G. F.; Tsvirko, M. P., Delayed fluorescence from the upper excited electronic states of metalloporphyrins. *Optics and Spectroscopy* **1980,** *49*, 278-281.
30. Stelmakh, G. F.; Tsvirko, M. P., METALLOPORPHYRIN DIMERIC S2 EMISSION RESULTING FROM TRIPLET-TRIPLET ANNIHILATION. *Acs Symposium Series* **1986,** *321*, 118-127.
31. Tripathy, U.; Steer, R. P., The photophysics of metalloporphyrins excited in their Soret and higher energy UV absorption bands. *Journal of Porphyrins and Phthalocyanines* **2007,** *11* (3-4), 228-243.
32. Sugunan, S. K.; Tripathy, U.; Brunet, S. M. K.; Paige, M. F.; Steer, R. P., Mechanisms of Low-Power Noncoherent Photon Upconversion in Metalloporphyrin-Organic Blue Emitter Systems in Solution. *Journal of Physical Chemistry A* **2009,** *113* (30), 8548-8556.
33. Singh-Rachford, T. N.; Castellano, F. N., Photon upconversion based on sensitized triplet-triplet annihilation. *Coordination Chemistry Reviews* **2010,** *254* (21-22), 2560-2573.
34. Schmidt, T. W.; Castellano, F. N., Photochemical Upconversion: The Primacy of Kinetics. *Journal of Physical Chemistry Letters* **2014,** *5* (22), 4062-4072.
35. Ravetz, B. D.; Pun, A. B.; Churchill, E. M.; Congreve, D. N.; Rovis, T.; Campos, L. M., Photoredox catalysis using infrared light via triplet fusion upconversion. *Nature* **2019,** *565* (7739), 343-346.
36. Glaser, F.; Kerzig, C.; Wenger, O. S., Multi-Photon Excitation in Photoredox Catalysis: Concepts, Applications, Methods. *Angewandte Chemie-International Edition* **2020,** *59* (26), 10266-10284.
37. Harriman, A., Luminescence of porphyrins and metalloporphyrins. Part 1.—Zinc(II), nickel(II) and manganese(II) porphyrins. *Journal of the Chemical Society, Faraday Transactions 1: Physical Chemistry in Condensed Phases* **1980,** *76* (0), 1978-1985.
38. Quimby, D. J.; Longo, F. R., Luminescence studies on several tetraarylporphins and their zinc derivatives. *Journal of the American Chemical Society* **1975,** *97* (18), 5111-5117.
39. Demchenko, A. P.; Tomin, V. I.; Chou, P. T., Breaking the Kasha Rule for More Efficient Photochemistry. *Chemical Reviews* **2017,** *117* (21), 13353-13381.
40. O'Brien, J. A.; Rallabandi, S.; Tripathy, U.; Paige, M. F.; Steer, R. P., Efficient S-2 state production in ZnTPP-PMMA thin films by triplet-triplet annihilation: Evidence of solute aggregation in photon upconversion systems. *Chemical Physics Letters* **2009,** *475* (4-6), 220-222.

41. Suppan, P.; Vauthey, E., The energy balance of photoinduced electron transfer reactions. *Journal of Photochemistry and Photobiology A: Chemistry* **1989,** *49* (1), 239-248.
42. Ramamurthy, P.; Parret, S.; Morletsavary, F.; Fouassier, J. P., Spin—orbit-coupling-induced triplet formation of triphenylpyrylium ion: a flash photolysis study. *Journal of Photochemistry and Photobiology a-Chemistry* **1994,** *83* (3), 205-209.
43. Velate, S.; Liu, X.; Steer, R. P., Does the radiationless relaxation of Soret-excited metalloporphyrins follow the energy gap law? *Chemical Physics Letters* **2006,** *427* (4-6), 295-299.
44. Harriman, A.; Porter, G.; Searle, N., Reversible photo-oxidation of zinc tetraphenylporphine by benzo-1,4-quinone. *Journal of the Chemical Society-Faraday Transactions Ii* **1979,** *75*, 1515-1521.
45. Kalyanasundaram, K., Photochemistry of polypyridine and porphyrin complexes. Academic Press: London ;, 1992.
46. Tyssee, D. A.; Baizer, M. M., Electrocarboxylation. I. Mono- and dicarboxylation of activated olefins. *Journal of Organic Chemistry* **1974,** *39* (19), 2819-2823.
47. Wolberg, A.; Manassen, J., Electrochemical and electron paramagnetic resonance studies of metalloporphyrins and their electrochemical oxidation products. *Journal of the American Chemical Society* **1970,** *92* (10), 2982-2991.
48. Mataga, N.; Shibata, Y.; Chosrowjan, H.; Yoshida, N.; Osuka, A., Internal conversion and vibronic relaxation from higher excited electronic state of porphyrins: Femtosecond fluorescence dynamics studies. *Journal of Physical Chemistry B* **2000,** *104* (17), 4001-4004.
49. Yu, H. Z.; Baskin, J. S.; Zewail, A. H., Ultrafast dynamics of porphyrins in the condensed phase: II. Zinc tetraphenylporphyrin. *Journal of Physical Chemistry A* **2002,** *106* (42), 9845-9854.
50. Hayes, R. T.; Walsh, C. J.; Wasielewski, M. R., Competitive Electron Transfer from the S2 and S1 Excited States of Zinc meso-Tetraphenylporphyrin to a Covalently Bound Pyromellitimide: Dependence on Donor−Acceptor Structure and Solvent. *The Journal of Physical Chemistry A* **2004,** *108* (13), 2375-2381.
51. Gurzadyan, G. G.; Tran-Thi, T. H.; Gustavsson, T., Time-resolved fluorescence spectroscopy of high-lying electronic states of Zn-tetraphenylporphyrin. *Journal of Chemical Physics* **1998,** *108* (2), 385-388.
52. Mataga, N.; Taniguchi, S.; Chosrowjan, H.; Osuka, A.; Kurotobi, K., Observations of the whole bell-shaped energy gap law in the intra-molecular charge separation (CS) from S-2 state of directly linked Zn-porphyrin-imide dyads: Examinations of wider range of energy gap (-Delta G(cs)) for the CS rates in normal regions. *Chemical Physics Letters* **2005,** *403* (1-3), 163-168.
53. Chosrowjan, H.; Tanigichi, S.; Okada, T.; Takagi, S.; Arai, T.; Tokumaru, K., Electron transfer quenching of S_2 state fluorescence of Zn-tetraphenylporphyrin. *Chemical Physics Letters* **1995,** *242* (6), 644-649.
54. Avramenko, A. G.; Rury, A. S., Quantum Control of Ultrafast internal Conversion Using Nanoconfined Virtual Photons. *Journal of Physical Chemistry Letters* **2020,** *11* (3), 1013-1021.
55. Liu, X.; Tripathy, U.; Bhosale, S. V.; Langford, S. J.; Steer, R. P., Photophysics of soret-excited tetrapyrroles in solution. II. Effects of perdeuteration, substituent nature and

position, and macrocycle structure and conformation in zinc(II) porphyrins. *Journal of Physical Chemistry A* **2008,** *112* (38), 8986-8998.
56. Ghosh, M.; Mora, A. K.; Nath, S.; Kumar, P. H.; Bangal, P. R.; Sinha, S., Photoinduced electron transfer from zinc tetraphenylporphyrin to 2-nitrofluorene in polar solvent acetonitrile. *Journal of Photochemistry and Photobiology a-Chemistry* **2015,** *306*, 55-65.
57. Morandeira, A.; Engeli, L.; Vauthey, E., Ultrafast charge recombination of photogenerated ion pairs to an electronic excited state. *Journal of Physical Chemistry A* **2002,** *106* (19), 4833-4837.
58. Tripathy, U.; Kowalska, D.; Liu, X.; Velate, S.; Steer, R. P., Photophysics of Soret-excited tetrapyrroles in solution. I. Metalloporphyrins: MgTPP, ZnTPP, and CdTPP. *Journal of Physical Chemistry A* **2008,** *112* (26), 5824-5833.
59. Su, W.; Singh, K.; Rogers, J.; Slagle, J.; Fleitz, P., The relationship of structure and optical properties of haloporphyrins: A new way to synthesize porphyrin chromophores and the investigation of their optical properties. *Materials Science and Engineering: B* **2006,** *132* (1), 12-15.
60. Moiseev, A. G.; Margulies, E. A.; Schneider, J. A.; Belanger-Gariepy, F.; Perepichka, D. F., Protecting the triplet excited state in sterically congested platinum porphyrin. *Dalton Transactions* **2014,** *43* (6), 2676-2683.
61. Murov, S. L.; Hug, G. L.; Carmichael, I., Handbook of photochemistry. **1993**.
62. Rodriguez, J.; Kirmaier, C.; Holten, D., Optical properties of metalloporphyrin excited states. *Journal of the American Chemical Society* **1989,** *111* (17), 6500-6506.
63. Pekkarinen, L.; Linschitz, H., Studies on Metastable States of Porphyrins .2. Spectra and Decay Kinetics of Tetraphenylporphine, Zinc Tetraphenylporphine and Bacteriochlorophyll. *Journal of the American Chemical Society* **1960,** *82* (10), 2407-2411.
64. Gou, L. J.; Coretsopoulos, C. N.; Scranton, A. B., Measurement of the dissolved oxygen concentration in acrylate monomers with a novel photochemical method. *Journal of Polymer Science Part a-Polymer Chemistry* **2004,** *42* (5), 1285-1292.
65. Montalti, M.; Credi, A.; Prodi, L.; Gandolfi, M. T., *Handbook of Photochemistry*. CRC Press: 2006.
66. Mongin, C.; Golden, J. H.; Castellano, F. N., Liquid PEG Polymers Containing Antioxidants: A Versatile Platform for Studying Oxygen-Sensitive Photochemical Processes. *Acs Applied Materials & Interfaces* **2016,** *8* (36), 24038-24048.
67. Zhou, Q. H.; Zhou, M. M.; Wei, Y. X.; Zhou, X. G.; Liu, S. L.; Zhang, S.; Zhang, B., Solvent effects on the triplet-triplet annihilation upconversion of diiodo-Bodipy and perylene. *Physical Chemistry Chemical Physics* **2017,** *19* (2), 1516-1525.
68. Lai, W. D.; Li, X. Z.; Liu, H. Q.; Han, L.; Zhao, Y. J.; Li, X. W., Interfacial Polycondensation Synthesis of Optically Sensitive Polyurea Microcapsule. *Journal of Chemistry* **2014**.
69. Oueslati, A.; Kamoun, S.; Hlel, F.; Gargouri, M.; Fort, A., Real-time FTIR monitoring of the photopolymerization of a pentaerythritol triacrylate-based resin. *Akademeia* **2011,** *1* (1).
70. Geuskens, G.; David, C., Identification of free radicals produced by the radiolysis of poly(methyl methacrylate) and poly(methyl acrylate) at 77°K. *Die Makromolekulare Chemie* **1973,** *165* (1), 273-280.

71. Sugiyama, Y., ESR studies on poly(methyl acrylate) radicals to estimate their dominant structure. *Chemistry Letters* **1996,** (11), 951-952.
72. Kunitake, T.; Murakami, S., Study of Radical Polymerizations by Spin Trapping .1. Trapping of Initiating and Propagating Radicals. *Polymer Journal* **1972,** *3* (2), 249-251.
73. Heitele, H.; Finckh, P.; Weeren, S.; Pollinger, F.; Michelbeyerle, M. E., Solvent polarity effects on intramolecular electron transfer. 1. Energetic aspects. *Journal of Physical Chemistry* **1989,** *93* (13), 5173-5179.
74. Gurzadyan, G. G.; Tran-Thi, T.-H.; Gustavsson, T., *Direct measurement of S2 -- S0 fluorescence lifetimes and anisotropy of tetraphenylporphyrins*. SPIE: 1999; Vol. 4060.
75. Lee, K. S.; Kim, R. H.; Yang, D. Y.; Park, S. H., Advances in 3D nano/microfabrication using two-photon initiated polymerization. *Progress in Polymer Science* **2008,** *33* (6), 631-681.
76. Vaezi, M.; Seitz, H.; Yang, S. F., A review on 3D micro-additive manufacturing technologies. *International Journal of Advanced Manufacturing Technology* **2013,** *67* (5-8), 1721-1754.

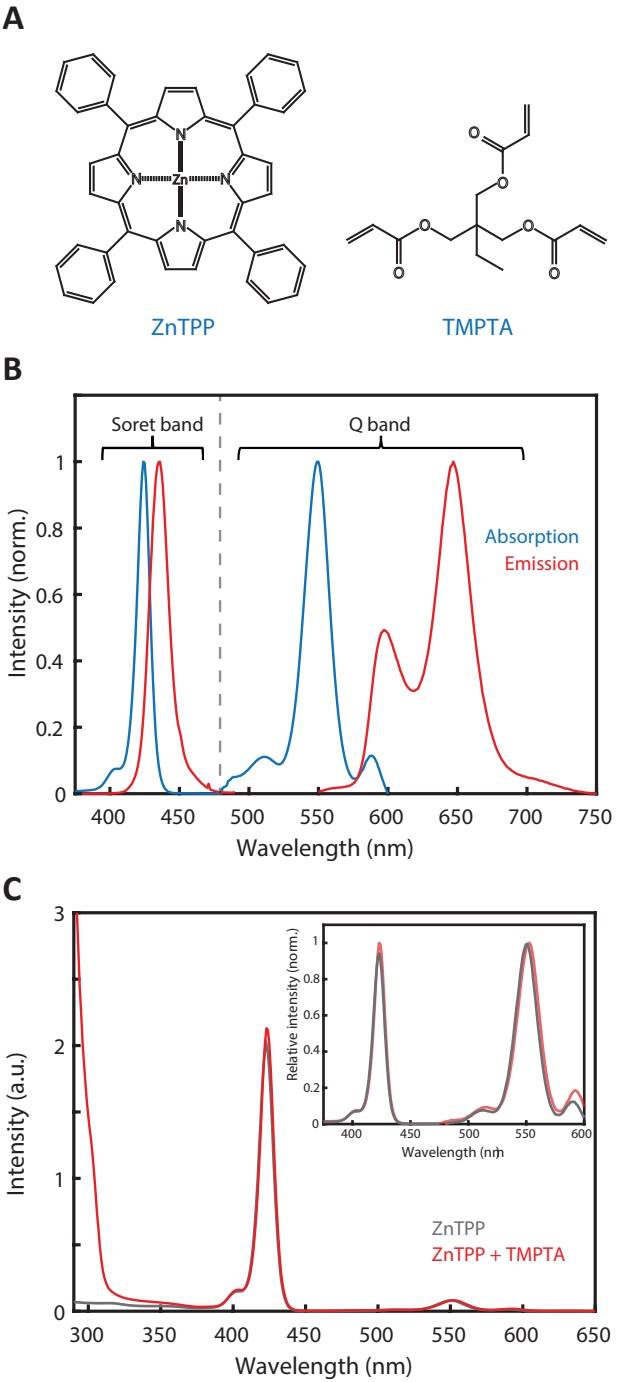
A
ZnTPP
TMPTA
B
Soret band
Q band
Absorption
Emission
Intensity (norm.)
Wavelength (nm)
C
Intensity (a.u.)
Wavelength (nm)
Relative intensity (norm.)
ZnTPP
ZnTPP + TMPTA

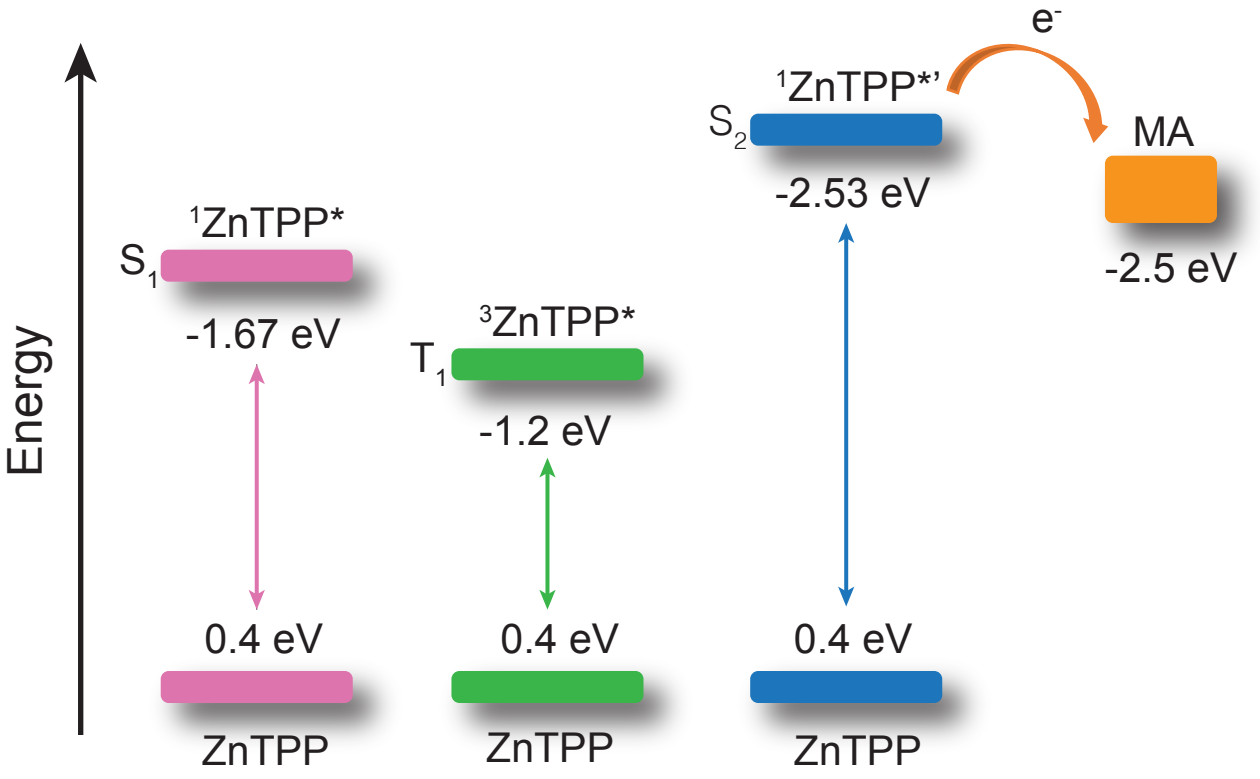
Energy
^{1}ZnTPP*
S_1
-1.67 eV
0.4 eV
ZnTPP
^{3}ZnTPP*
T_1
-1.2 eV
0.4 eV
ZnTPP
^{1}ZnTPP*'
S_2
-2.53 eV
0.4 eV
ZnTPP
e$^-$
MA
-2.5 eV

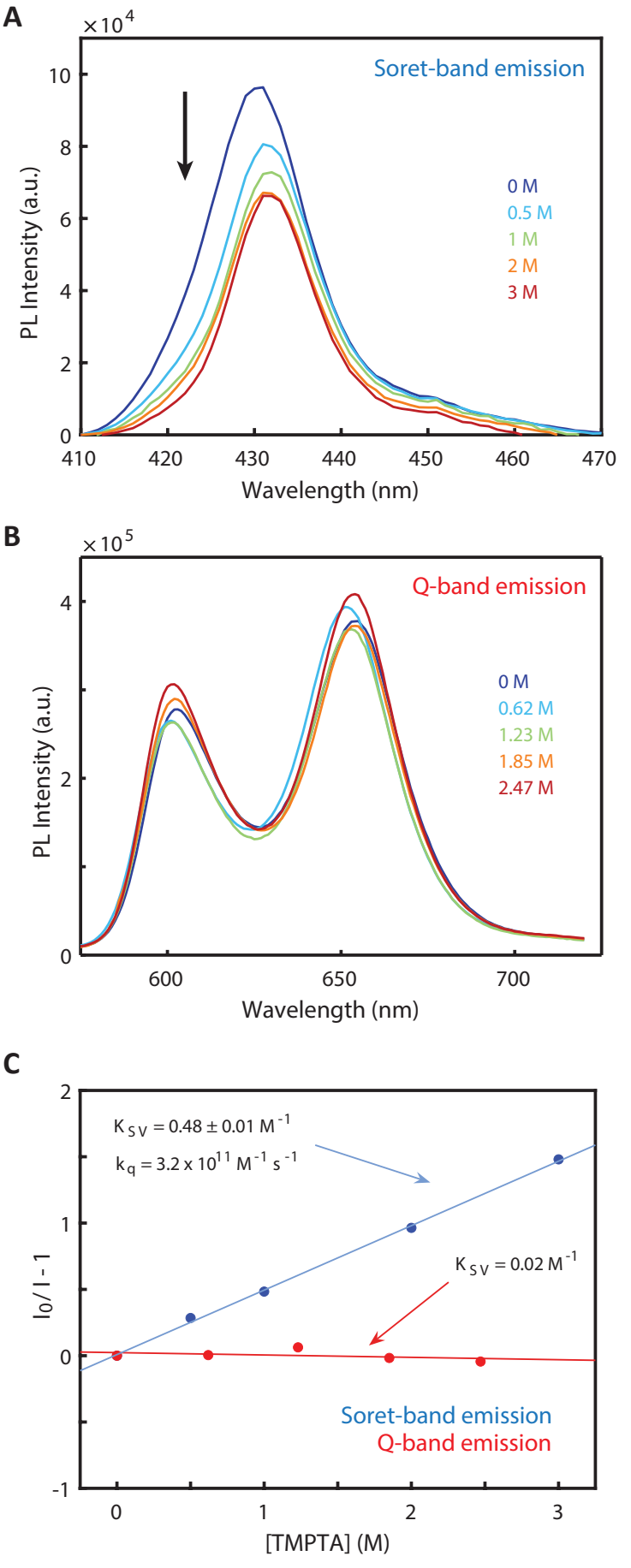
A
×10^4
Soret-band emission
PL Intensity (a.u.)
0 M
0.5 M
1 M
2 M
3 M
Wavelength (nm)
B
×10^5
Q-band emission
PL Intensity (a.u.)
0 M
0.62 M
1.23 M
1.85 M
2.47 M
Wavelength (nm)
C
K SV = 0.48 ± 0.01 M^-1
k q = 3.2 x 10^11 M^-1 s^-1
K SV = 0.02 M^-1
Soret-band emission
Q-band emission
I0/ I - 1
[TMPTA] (M)

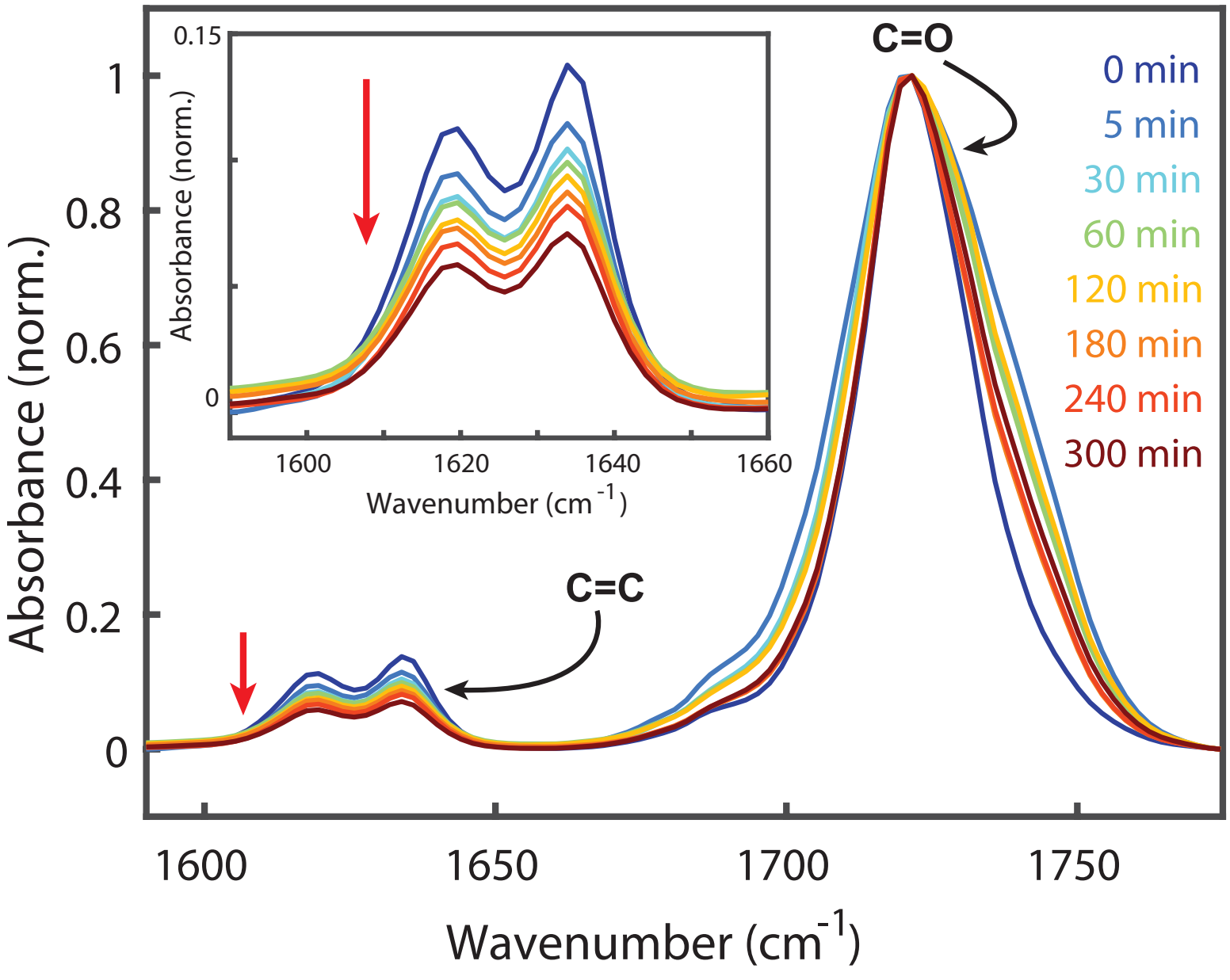
Absorbance (norm.)
Wavenumber (cm-1)
C=O
C=C
0 min
5 min
30 min
60 min
120 min
180 min
240 min
300 min
0.15
0
Absorbance (norm.)
1600
1620
1640
1660
Wavenumber (cm-1)

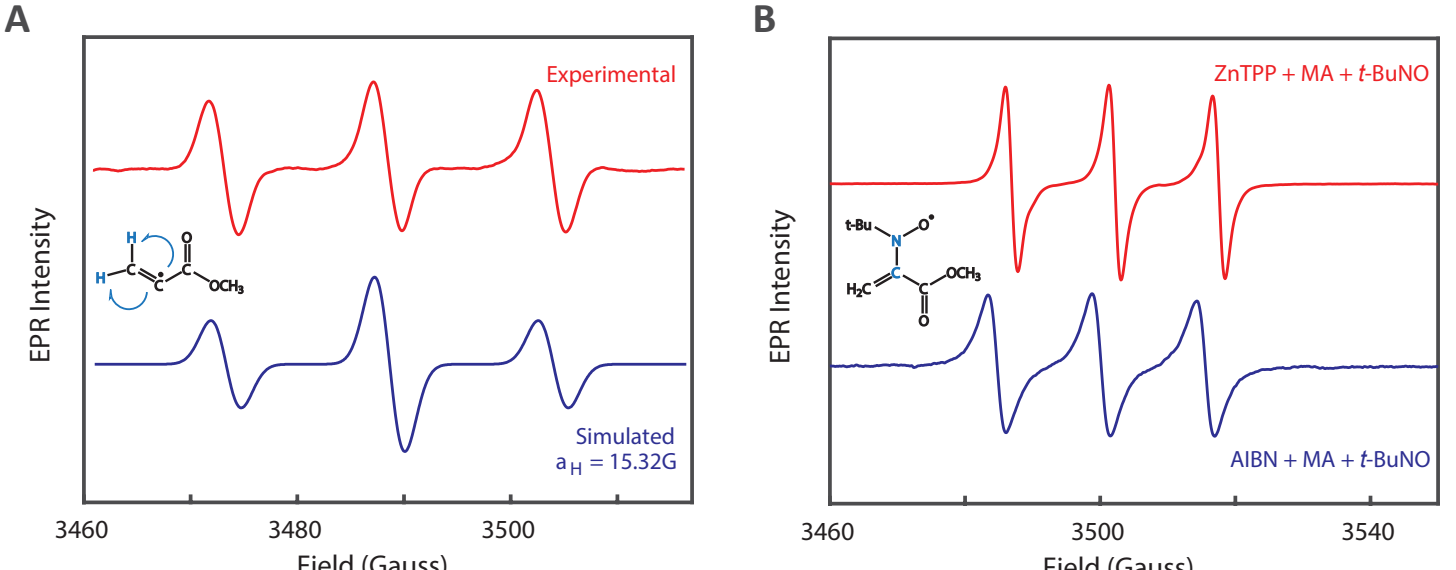
A
Experimental
Simulated
a_H = 15.32G
EPR Intensity
3460
3480
3500
Field (Gauss)
B
ZnTPP + MA + t-BuNO
AIBN + MA + t-BuNO
EPR Intensity
3460
3500
3540
Field (Gauss)

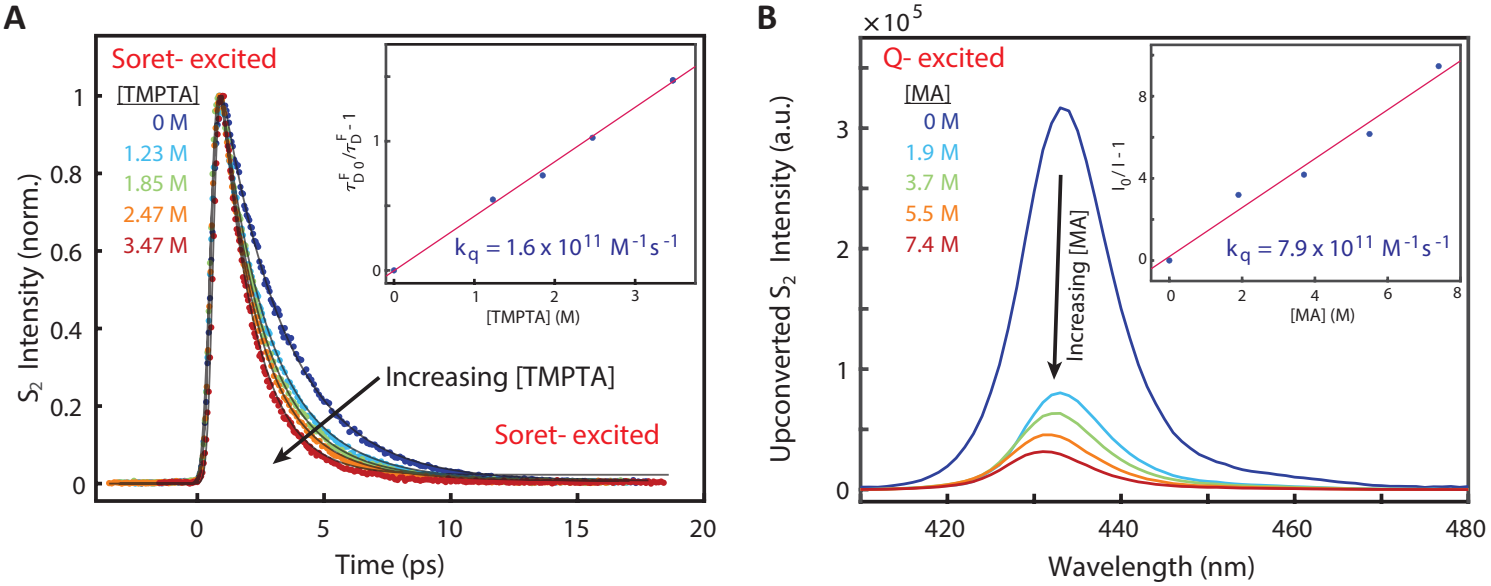
A
Soret- excited
[TMPTA]
0 M
1.23 M
1.85 M
2.47 M
3.47 M
S2 Intensity (norm.)
Time (ps)
Increasing [TMPTA]
Soret- excited
τF D 0 /τF D -1
[TMPTA] (M)
kq = 1.6 x 10^11 M^-1s^-1
B
×10^5
Q- excited
[MA]
0 M
1.9 M
3.7 M
5.5 M
7.4 M
Upconverted S2 Intensity (a.u.)
Wavelength (nm)
Increasing [MA]
I0/I - 1
[MA] (M)
kq = 7.9 x 10^11 M^-1s^-1

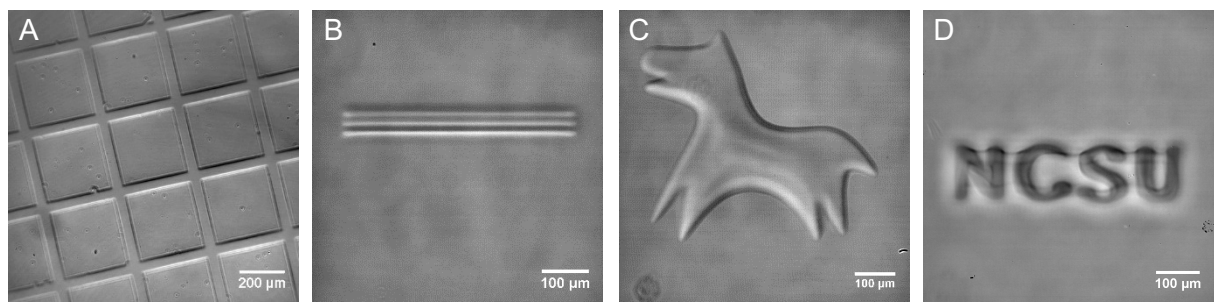
A
200 µm
B
100 µm
C
100 µm
D
NCSU
100 µm